AL/CF-TR-1995-0043

ARMSTRONG LABORATORY

CORIOLIS STUDY OF THE DYNAMIC ENVIRONMENT SIMULATOR

Daniel W. Repperger

CREW SYSTEMS DIRECTORATE
BIODYNAMICS AND BIOCOMMUNICATIONS DIVISION
WRIGHT-PATTERSON AFB OH 45433-7008

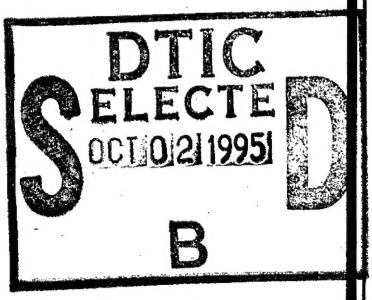

APRIL 1995

19950928 007

FINAL REPORT FOR THE PERIOD OCTOBER 1990 TO APRIL 1995

Approved for public release; distribution is unlimited

DTIC QUALITY INSPECTED 5

AIR FORCE MATERIEL COMMAND
WRIGHT-PATTERSON AIR FORCE BASE, OHIO 45433-6573

NOTICES

When US Government drawings, specifications, or other data are used for any purpose other than a definitely related Government procurement operation, the Government thereby incurs no responsibility nor any obligation whatsoever, and the fact that the Government may have formulated, furnished, or in any way supplied the said drawings, specifications, or other data, is not to be regarded by implication or otherwise, as in any manner licensing the holder or any other person or corporation, or conveying any rights or permission to manufacture, use, or sell any patented invention that may in any way be related thereto.

Please do not request copies of this report from the Armstrong Laboratory. Additional copies may be purchased from:

National Technical Information Service
5285 Port Royal Road
Springfield, Virginia 22161

Federal Government agencies registered with the Defense Technical Information Center should direct requests for copies of this report to:

Defense Technical Information Center
Cameron Station
Alexandria, Virginia 22314

TECHNICAL REVIEW AND APPROVAL

AL/CF-TR-1995-0043

This report has been reviewed by the Office of Public Affairs (PA) and is releasable to the National Technical Information Service (NTIS). At NTIS, it will be available to the general public, including foreign nations.

This technical report has been reviewed and is approved for publication.

FOR THE DIRECTOR

Thomas J Moore

THOMAS J. MOORE, Chief
Biodynamics and Biocommunications Division
Armstrong Laboratory

REPORT DOCUMENTATION PAGE

Form Approved
OMB No. 0704-0188

Public reporting burden for this collection of information is estimated to average 1 hour per response, including the time for reviewing instructions, searching existing data sources, gathering and maintaining the data needed, and completing and reviewing the collection of information. Send comments regarding this burden estimate or any other aspect of this collection of information, including suggestions for reducing this burden, to Washington Headquarters Services, Directorate for Information Operations and Reports, 1215 Jefferson Davis Highway, Suite 1204, Arlington, VA 22202-4302, and to the Office of Management and Budget, Paperwork Reduction Project (0704-0188), Washington, DC 20503.

1. AGENCY USE ONLY *(Leave blank)*	2. REPORT DATE	3. REPORT TYPE AND DATES COVERED
	April 1995	Final - October 1990 to April 1995

4. TITLE AND SUBTITLE

Coriolis Study of the Dynamic Environment Simulator

5. FUNDING NUMBERS

PE - 0601101F
PR - ILIR
TA - ILIRBB
WU - ILIRBB13

6. AUTHOR(S)

Daniel W. Repperger

7. PERFORMING ORGANIZATION NAME(S) AND ADDRESS(ES)

Armstrong Laboratory, Crew Systems Directorate
Biodynamics and Biocommunications Division
Human Systems Center
Air Force Materiel Command
Wright-Patterson AFB OH 45433-7022

8. PERFORMING ORGANIZATION REPORT NUMBER

AL/CF-TR-1995-0043

9. SPONSORING/MONITORING AGENCY NAME(S) AND ADDRESS(ES)

10. SPONSORING/MONITORING AGENCY REPORT NUMBER

11. SUPPLEMENTARY NOTES

12a. DISTRIBUTION/AVAILABILITY STATEMENT

Approved for public release; distribution is unlimited

12b. DISTRIBUTION CODE

13. ABSTRACT *(Maximum 200 words)*

A three axis motion simulator is modeled as a robotic manipulator. The equations of motion are derived and the terms due to Coriolis are quantified. Two optimization algorithms are presented to minimize the Coriolis produced in the simulator at the end effector. It is shown with minimal reduction of motion fidelity, that over 65 percent of Coriolis can be reduced with proper input commands to modify the motion field produced. When this reduction of Coriolis is realized, the motion fidelity is only compromised about 5 percent which may not be perceivable by the human subjects that participate in the human runs in the mechanical system considered herein.

14. SUBJECT TERMS	15. NUMBER OF PAGES
Motion Simulator, Mathematical Modeling, Coriolis Accelerations	30
	16. PRICE CODE

17. SECURITY CLASSIFICATION OF REPORT	18. SECURITY CLASSIFICATION OF THIS PAGE	19. SECURITY CLASSIFICATION OF ABSTRACT	20. LIMITATION OF ABSTRACT
UNCLASSIFIED	UNCLASSIFIED	UNCLASSIFIED	UNLIMITED

THIS PAGE LEFT BLANK INTENTIONALLY.

PREFACE

The Dynamic Environment Simulator (DES) is a three axes centrifuge device which has been used to replicate agile flight or supermaneuvers that an aircraft may fly in a combat scenario. In order to simulate these maneuvers, it requires the centrifuge to utilize simultaneous multiaxes motion. In this device, a pilot will sit on the seat in the third and innermost gimbal (the cab) and be subjected to simultaneous three axes motion. As all three axes rotate, the subject will not only experience the motion programmed to emulate the supermaneuver, but also experience motion fields generated by Coriolis components. These Coriolis components produce unusual and unnatural accelerations (which induce forces) and reduce the credibility of the motion simulation to emulate the true flight scenario.

Coriolis accelerations are a natural property arising from physics and dynamics and occur whenever a coordinate frame moves relative to another moving coordinate frame. The DES is a physical system and, as such, each gimbal is connected to another supporting gimbal. Thus the very nature of the physical construction of the DES provides a framework to produce Coriolis type accelerations.

In order to work on a means of reducing the Coriolis action produced by the centrifuge motion simulator, the first step is to accurately define the equations of motion of the DES. Once these equations of motion are obtained, one can then extract those terms that contribute only to the Coriolis component. Knowing these terms, the next step is to minimize their magnitude by inserting into the commands of the actuators an additional signal to drive the centrifuge simulator in such a manner as to mitigate these untoward effects. This minimization of Coriolis components also has a price in that it compromises the other commands inserted into the actuators, thereby affecting the total motion field produced. Thus it is necessary to both characterize the extent of the motion field action caused by the Coriolis accelerations as well as when this action is minimized. Consequently, it is also necessary to quantify the impact of the minimization of the Coriolis on the overall credibility of the motion simulation.

To minimize the Coriolis effects, an optimization procedure is given in this report which allows the Control Engineer the opportunity to insert appropriate input commands into the actuators of the centrifuge simulator. These input commands turn out to have a special feedback nature which not only provides both a method to accurately control a mechanical system such as the DES, but also allows the monitoring and regulation of the response of this motion simulator.

Accession For	
NTIS GRA&I	☑
DTIC TAB	☐
Unannounced	☐
Justification	
By	
Distribution/	
Availability Codes	
Dist	Avail and/or Special
A-1	

THIS PAGE LEFT BLANK INTENTIONALLY.

TABLE OF CONTENTS

LIST OF FIGURES

LIST OF TABLES

INTRODUCTION

The DES (Dynamic Environment Simulator) is a three axes centrifuge simulator which can be used to emulate motion fields as experienced in agile or supermaneuverable aircraft [1,2]. Figure 1 illustrates a schematic diagram of this mechanical system. In order to generate complex motions that appear in such flight scenarios, one or more axes of the DES must be operated simultaneously to develop the desired motion field profile to appear at the seat located within the cab depicted in Figure 1.

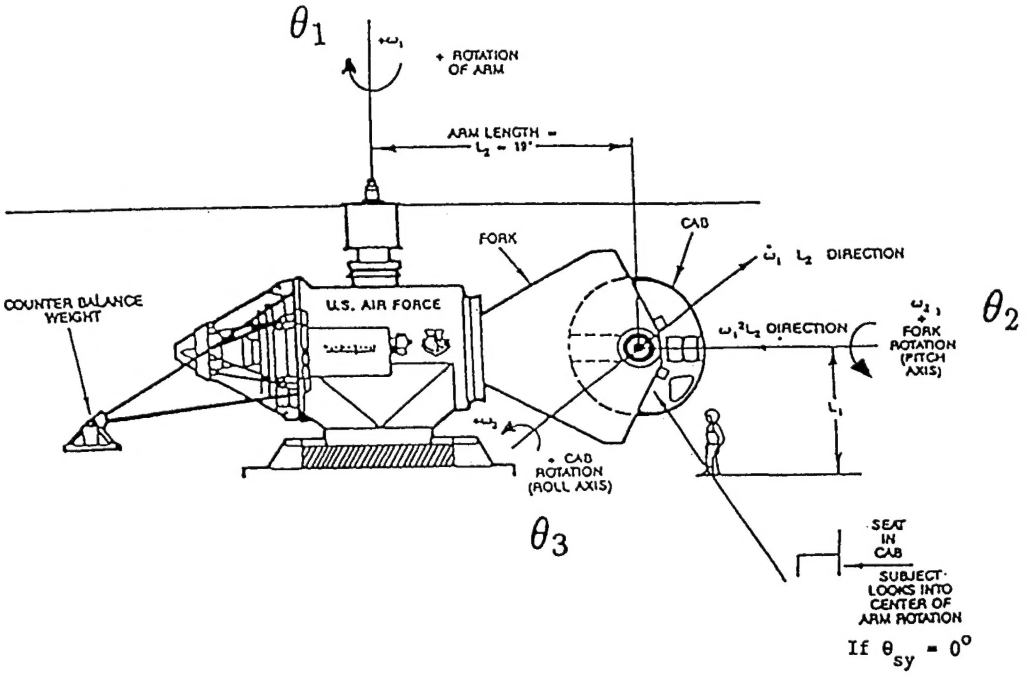

Figure 1. A Schematic Diagram of the DES

When a coordinate frame moves relative to another moving frame (which occurs in the DES since the physical gimbals are interconnected to one another), this may introduce Coriolis acceleration components. What is unusual about the Coriolis induced components are that they act in a direction perpendicular to normal induced accelerations and motion. When humans are exposed to such phenomena, they feel these motions are very unrealistic since the forces they experience are orthogonal to the direction of movement. Since the goal in motion simulation is to generate both linear and angular accelerations that feel realistic, the Coriolis component is detrimental to the production of good motion in a perceptual sense.

The purpose of this study is to first quantify the Coriolis component of the motion produced in the DES. Secondly, it is desired to work on a means of reducing this effect without too much compromise of the other motions that are chosen to be emulated. First an argument is made on the existence of such motions as Coriolis and some examples are given to illustrate this natural artifact of relative motion. These motions are then quantified, and then a means

of reducing such motions is suggested. A computer simulation demonstrates the extent of the reduction of the Coriolis component by the algorithms employed herein. We first discuss the existence of such untoward motions and how they are a natural product of the physics and dynamics of mechanical systems such as the DES.

Definition of Coriolis

The classical definition of Coriolis acceleration is well-known since its early definition by the French mathematician, G. Coriolis. The first example in this report is used to define Coriolis in a classical sense.

Example 1 - The Classical Definition of Coriolis

If a bar rotates (Figure 2) with an angular velocity W which has a vector direction out of the paper and a slider moves along the arm with linear velocity V, the action of the Coriolis acceleration $a_{(Coriolis)}$ which is induced on the slider satisfies the vector cross product relationship:

$$a_{(Coriolis)} = 2 \; W \; X \; V \qquad (1)$$

where $a_{(Coriolis)}$ is in a direction orthogonal to both the arm and the W vector as indicated in Figure 2. If a human subject were positioned on the slider on the rotating arm, and were to make any body motion in the direction of the slider movement (V), an acceleration $a_{(Coriolis)}$ would act on the subject in the direction of $a_{(Coriolis)}$ as depicted in Figure 2. This is very counterintuitive for a human subject to experience an acceleration (or resulting force) on his body acting in this direction, orthogonal to the moving slider.

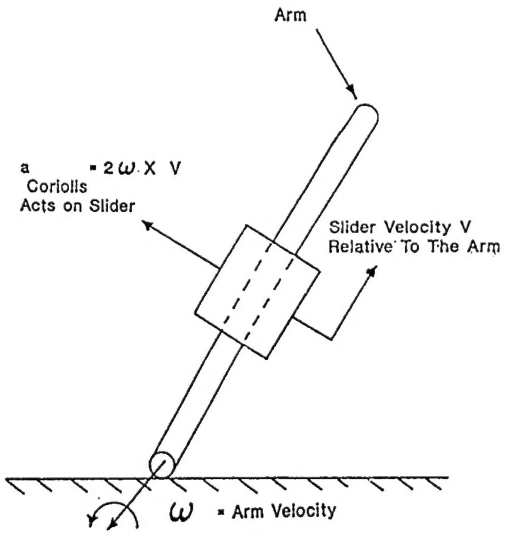

Figure 2. The Classical Definition of Coriolis

More specifically, if a human subject were positioned on the arm with his head closest to the center of rotation, and if he were to extend his arm radially outward, a force would be felt to his left side. If he reverses this motion, he feels a force to the right. This is also very counterintuitive because the directions change. For further discussion, use will be made of Figure 3 which illustrates the body centered coordinate system notation normally applied in sustained acceleration studies and will be adopted as the reference frame in this report.

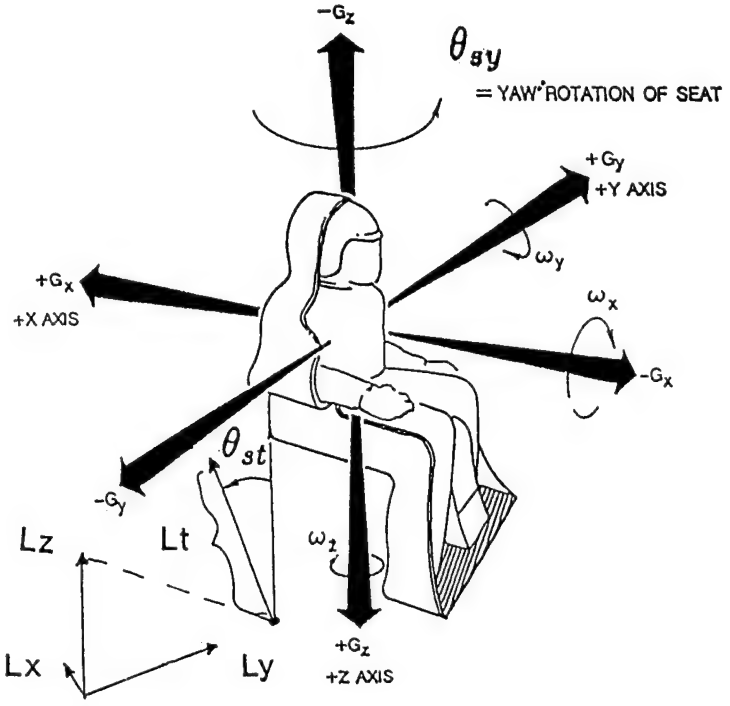

Figure 3. The Body Axis Coordinate System

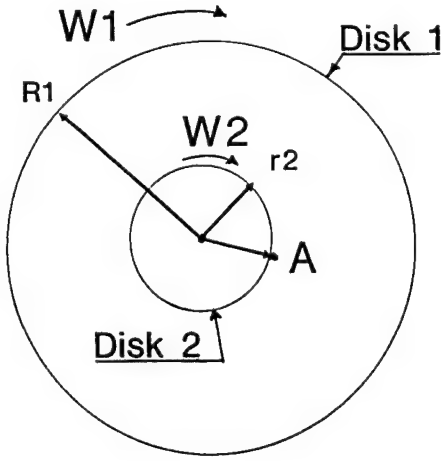

Figure 4. The Two Disk Example to Mathematically Derive Coriolis

A second example is now given which illustrates a mathematical basis why Coriolis accelerations always appear on systems where a frame experiences movement relative to another ambulatory frame (usually inertial).

Example 2 - The Mathematical Basis of Coriolis Motion

Figure 4 depicts an example from dynamics which provides a clear mathematical understanding of the origin of Coriolis accelerations and their subsequent forces. In Figure 4, the large disk (Disk 1) of radius R1 rotates at angular velocity W1. The smaller disk (Disk 2) of radius r2 has the same center and rotates at angular velocity W2 relative to Disk 1. It is desired to calculate the accelerations appearing at the point A on the smaller disk. The centripetal acceleration acting at a point moving in a circle is given by:

$$\text{acceleration}_{(\text{centripetal})} = \text{Radius} * W^2 \qquad (2)$$

For simplicity, this example will assume W1 and W2 are constant, thus eliminating any tangential component of acceleration appearing. Hence, the centripetal acceleration is the main acceleration of interest at the point A. Since both disks rotate about the same center and the smaller disk rotates on top of the larger disk, the total angular velocity of point A with respect to the inertial frame is W1 + W2. There are two ways to attempt to calculate the net radial acceleration appearing at point A.

Method 1 - Attempt to Add the Accelerations Linearly

At first glance, one may try to add the two accelerations separately in a linear manner by taking into account the movement of both bodies. Proceeding in this manner, the acceleration induced on point A by the larger disk would be given by:

$$\text{centripetal acceleration due to Disk 1} = r2\ W1^2 \qquad (3)$$

since the point A is r2 units from the center of rotation of disk 1. Next, one would calculate the acceleration induced at point A due to the rotation of the smaller disk.

$$\text{centripetal acceleration due to Disk 2} = r2\ W2^2 \qquad (4)$$

Thus, if this procedure is followed, the total acceleration acting on point A would be erroneously calculated as:

$$\text{total acceleration on point A} = r2\ W1^2 + r2\ W2^2 \qquad (5)$$

This is not correct because the Coriolis effects have been neglected. The missing Coriolis term is:

$$\text{missing Coriolis term} = 2 * W1\ r2\ W2 \qquad (6)$$

and acts in a radial direction on the smaller disk at point A. To see how this missing term arises, the correct solution to this problem is now presented to illustrate its origin.

Method 2 - Calculation of Accelerations from the Inertial Frame

If one now views the system in Figure 4 from an inertial frame perspective, the point A has a total angular velocity of W1 + W2. Thus, the calculation of the total radial acceleration acting on the point A is given by:

$$\text{total centripetal acceleration of point A} = (W1+W2)^2 * r2 \qquad (7)$$

This differs from the solution given in equation (5) but is the correct result. With some study, the missing term can be attributed to the fact that:

$$W1^2 + W2^2 \text{ is not equal to } (W1 + W2)^2 \qquad (8)$$

Thus, Coriolis accounts for the cross term which is missing when the square of the sum differs from the sum of the squares. This difference, however, may comprise a very significant part of the calculation of the total acceleration that appears at point A.

There are some situations in which it is physically possible to experience the untoward artifact of Coriolis accelerations. Figure 5 illustrates a simple playground device for children which enables anyone to perceive this variable and validate its existence. If the device rotates counter clockwise and a subject sits (looking inward) on the rim of the apparatus making an arm or foot movement radially inward will result in an experience of an acceleration (and force) to the subject's left. Conversely, making an arm or foot movement radially outward will result in an experience of an acceleration (and force) to the right. If the direction of rotation of the playground device is reversed, opposite accelerations and forces are perceived.

Finally, the use of the term "Coriolis" should be distinguished from its common usage occurring in studies on spatial orientation. This has a different meaning and refers to an illusion or misperception of attitude information. For example, from a subject's perspective, if he moves his head out of one plane of rotation and into another, as can occur on a human centrifuge, the semi-circular canals of the human vestibular system can be excited in such a manner as to elicit conflicting motion cues. The "Coriolis illusion," as it is called, is reduced in pilots by having them restrict head motions while their aircraft is turning or accelerating. Reference [3] addresses the detection of such illusory phenomenon.

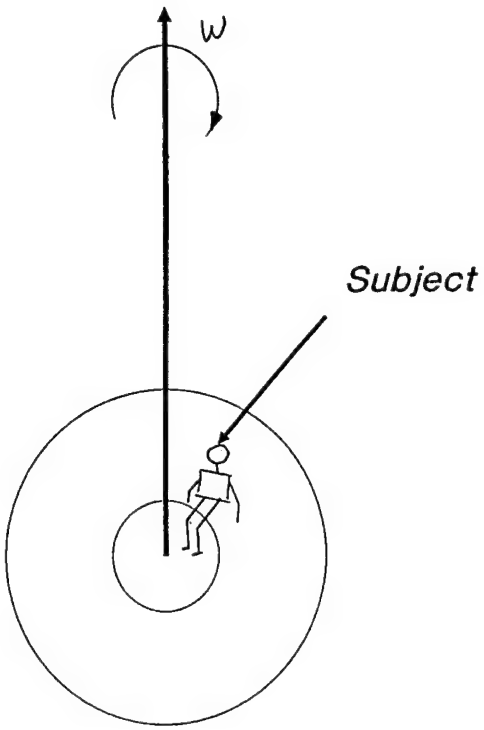

Figure 5. A Physical System To Experience Coriolis Acceleration

The Coriolis artifact just described is significantly larger in a motion simulator as compared to the actual aircraft because the turn radius difference is two orders of magnitude larger in the aircraft as compared to the simulator. This type of motion mismatch degrades the fidelity of the motion simulator considered herein and limits its use to very restricted motion studies. It is desired in this report to modify the joint commands into the actuators of the simulator to eliminate, or at least reduce, some of these Coriolis accelerations which are produced in the ground base motion simulator. In this manner the motion simulator will produce a motion field which is more credible to human subjects, yet utilize the full capability of the multi axes system of the centrifuge motion simulator.

The next step is to describe the DES in more explicit detail and then derive the equations of motion.

The Dynamic Environment Simulator (DES)

The approach taken here will be to model this mechanical system within the context of a robotic system. This is due to many new developments in the study of robotic manipulators that will help in the determination of the Coriolis terms that appear in the equations of motion.

If one wishes to model a three axes centrifuge simulator as a robotic system (Figure 1), one approach is to assume the centrifuge is a multiple link system with three revolute axes in which each axis rotates 360 degrees. The human (a pilot involved in an experiment of unusual acceleration stress or rotations) sits at the end effector (seat in the cab) and his body is subjected to the induced motion field. When modeling a centrifuge simulator as a robotic system, the main distinction between this problem and a traditional robotics problem involves the size of the mechanical system which, in this case, is prohibitively large (over 24 feet in height and over 180 tons in weight) with a work volume exceeding $9x10^3$ feet^3.

Once this problem is defined within the context of a robotic system, the forward and inverse kinematics problems which help define the equations of motion can be obtained using standard Denavit-Hartenberg formulation. As a first step, it is required to classify all centrifuge parameters (both fixed and rotating quantities) that will influence the equations of motion, and thus the calculated Coriolis induced accelerations.

Table 1 illustrates the physical parameters of the centrifuge simulator depicted in Figure 1. The last six fixed variables (L_x,L_y,L_z,L_t, Θ_{sy}, and Θ_{st}) refer to the seat in the cab displayed in Figures 1 and 3.

Table 1. Fixed and Rotational Parameters of the DES

Fixed Variable	Dimensions	Rotational Variable	Max	Min	Dimensions
L_1	12.27 Feet	Θ_1	2 Pi	-2 Pi	rad.
L_2	19.0 Feet	$\dot{\Theta}_1$	5.86	-5.86	rad/s
L_x	3.90 Feet	$\ddot{\Theta}_2$	0.63	-0.63	rad/s/s
L_y	0.012 Feet	Θ_2	2 Pi	-2.0 Pi	rad
L_z	0.012 Feet	$\dot{\Theta}_2$	3.14	- Pi	rad/s
L_t	2.76 Feet	$\ddot{\Theta}_2$	2.5	-2.5	rad/s/s
Θ_{sy}	$0<\Theta_{sy}<2$ Pi rad	Θ_3	2 Pi	-2 Pi	rad
Θ_{st}	$0<\Theta_{st}<$Pi/2 rad	$\dot{\Theta}_3$	3.14	-3.14	rads/s
		$\ddot{\Theta}_3$	5.0	-5.0	rad/s/s

where Pi=3.1416, Θ_1 (arm), Θ_2 (fork), and Θ_3 (cab) are the three revolute joints. The variables Θ_{sy} and Θ_{st} refer to rotations of the pilot's seat (yaw and pitch) at the end effector. The variables L_1 and L_2 refer to centrifuge link lengths; the variables L_x, L_y, L_z, and L_t refer to link lengths associated with the pilot's seat at the end effector (cf. Figures 1,3).

From a pilot's perspective, if the seat is configured in the tangential direction (Θ_{sy} = Pi/2 radians), the traditional roll, pitch, and yaw angles would be specified by: roll = Θ_3, pitch = - Θ_2, and yaw = Θ_{sy}. It is also important, in describing the DES as a robotic manipulator, to clarify how the controlling action of the different axes is achieved.

The Control Characteristics of the Device

The first axis in Figure 1 (the arm described by the axis Θ_1 or W1) is a velocity control system driven by three electric motors physically connected in tandem. Thus, velocity command inputs are compared to the angular velocity (tachometer) measurement of the actual arm speed producing a velocity error. Acting in a feedback manner, this velocity error is multiplied by a gain and this signal augments the torque produced for that axis to drive the attained velocity to the command signal. The second axis (the fork with axis Θ_2) is actuated by a separate DC electric motor but is a position control system. In this case, the input consists of position command signals (voltages) and position measurements are obtained from a pair of resolvers, thus delivering a position error for use in a controller design. The third axis (the cab with axis Θ_3) is also a position control system, but is actuated by a hydraulic motor and has similar operation to the fork control system.

In order to specify the actual motion produced by the flight simulator, the kinematics aspects of this manipulator are now described in more specific detail.

The Kinematic Description of the DES

In [1] a description of the forward kinematics of this mechanical system was derived using the frame assignments (Denevit-Hartenberg) from Craig [4]. This detailed derivation involving a total of 17 coordinate systems was used to display many different possible seat orientations and translations as illustrated in Table 2. The purpose of using such a large number of coordinate frames in this analysis of the manipulator system was to have additional freedom to investigate possible optimization of the system's configuration parameters.

Other kinematic derivations are much simpler, e.g. [5] and are useful for other situations. We display here the parameters obtained by viewing the DES within the context of a robotic manipulator system using the full Denevit-Hartenberg formulation.

Table 2. The Denavit-Hartenberg Parameters For The DES

Angle Link i	From zi-1 to zi about Xi-1 = ai-1	Distance Along zi-1 to zi along Xi-1 = Ai-1	Distance Along Xi-1 to Xi along Zi = di	Angle From Xi-1 to Xi about Zi = Θ_i
1	0	0	0	$-\Theta_1$
2	0	L2	0	0
3	0	0	0	Pi/2
4	Pi/2	0	0	0
5	0	0	0	Θ_2
6	0	0	0	Pi/2
7	-Pi/2	0	0	0
8	0	0	0	Θ_3
9	0	-Lx	+Lz	0
10	0	0	0	- Pi/2
11	0	Ly	0	0
12	Pi/2	0	0	0
13	0	0	0	$-\Theta_{sy}$
14	-Pi/2	0	0	0
15	0	0	0	$-\Theta_{st}$
16	Pi/2	0	0	0
17	0	0	-Lt	0

The transformation matrix T_0^{17} relating the inertial frame to the seventeenth coordinate system can be derived (cf. [6]):

$$T_0^{17} = \begin{matrix} T_{11}, T_{12}, T_{13}, T_{14} \\ T_{21}, T_{22}, T_{23}, T_{24} \\ T_{31}, T_{32}, T_{33}, T_{34} \\ T_{41}, T_{42}, T_{43}, T_{44} \end{matrix} \qquad (9)$$

where T_0^{17} is the Denevit-Hartenberg transformation used, e.g. in [4], with relevant components:

$$T_{11} = s1\ c2\ s_{(sy)}\ c_{(st)} + s1\ s2\ c3\ s_{(st)}$$
$$-s1\ s2\ s3\ c_{(sy)}\ c_{(st)} + c1\ s3\ s_{(st)} + c1c3c_{(sy)}c_{(st)} \qquad (10a)$$

$$T_{12} = -s1\ c2\ c_{(sy)} - s1\ s2\ s3\ s_{(sy)} + c1\ c3\ s_{(sy)} \qquad (10b)$$

$$T_{13} = -s1\ c2\ s_{(sy)}\ s_{(st)} + s1\ s2\ c3\ c_{(st)}$$
$$+ s1\ s2\ s3\ c_{(sy)}\ s_{(st)} + c1\ s3\ c_{(st)} - c1c3c_{(sy)}s_{(st)} \qquad (10c)$$

$$T_{14} = s1\ c2\ Lt\ s_{(sy)}\ s_{(st)} - Lz\ s1\ c2 - s1\ s2\ c3\ Lt\ c_{(st)}$$
$$-s1\ s2\ s3\ Lt\ c_{(sy)}\ s_{(st)} - s1\ s2\ Ly\ s3 - c1s3Ltc_{(st)}$$
$$+ c1\ Lx\ s3 + c1\ Lt\ c_{(sy)}\ s_{(st)}\ c3 + c1\ Lyc3 + c1\ L2 + Lxc3s1s2 \qquad (10d)$$

$$T_{21} = c1\ c2\ s_{(sy)}\ c_{(st)} + c1\ s2\ c3\ s_{(st)} - c1\ s2\ s3\ c_{(sy)}\ c_{(st)} - s1\ s3\ s_{(st)} - s1c3c_{(sy)}c_{(st)} \quad (10e)$$

$$T_{22} = - c1\ c2\ c_{(sy)} - c1\ s2\ s3\ s_{(sy)} - s1\ c3\ s_{(sy)} \quad (10f)$$

$$T_{23} = - c1\ c2\ s_{(sy)}\ s_{(st)} + c1\ s2\ c3\ c_{(st)} + c1\ s2\ s3\ c_{(sy)}\ s_{(st)} - s1\ s3\ c_{(st)} + s1c3c_{(sy)}s_{(st)} \quad (10g)$$

$$T_{24} = c1\ c2\ Lt\ s_{(sy)}\ s_{(st)} - c1\ c2\ Lz - c1s2c3\ Ltc_{(st)} + c1s2c3\ Lx - c1s2\ Lt\ c_{(sy)}s_{(st)}s3 - c1s2\ Lys3 + s1\ s3\ Lt\ c_{(st)} - s1\ Lx\ s3 - s1\ Lt\ s_{(st)}c3c_{(sy)} - Ly\ s1\ c3 - L2\ s1 \quad (10h)$$

$$T_{31} = s2\ s_{(sy)}\ c_{(st)} - c2\ c3\ s_{(st)} + c2\ s3c_{(sy)}c_{(st)} \quad (10i)$$

$$T_{32} = -s2\ c_{(sy)} + c2\ s3\ s_{(sy)} \quad (10j)$$

$$T_{33} = -s2\ s_{(sy)}\ s_{(st)} - c2\ c3\ c_{(st)} - c2\ s3c_{(sy)}s_{(st)} \quad (10k)$$

$$T_{34} = s2\ Lt\ s_{(sy)}\ s_{(st)} - s2\ Lz + c2\ c3\ Lt\ c_{(st)} - c2\ c3\ Lx + c2\ s3\ Lt\ c_{(sy)}\ s_{(st)} + c2\ Ly\ s3 \quad (10L)$$

where s and c refer to the standard sine and cosine notation and for the subscript notation, those terms with s refer only to the seat variables.

To complete the kinematic relationships, the relevant details used in the derivation can be briefly summarized as follows:

Forward Kinematic Relationships

Let X be a 3x1 position vector in Cartesian space and Θ a 3x1 joint space vector. The forward kinematics relationship between X and Θ can be specified via:

$$X = f(\Theta) \quad (11)$$

where the function f(.) [6] for a centrifuge motion simulator is an extremely complicated function of the 3 joint variables Θ_i, (i=1,3) and their derivatives. If X is a linear position vector and denoting its 3x1 dimensional velocity vector as V, then:

$$V = (d/dt)\ X = J1\ \ (d/dt)\ \Theta \quad (12)$$

as the linear velocity relationship and the dot or derivative indicates time differentiation. J1 is the 3x3 manipulator Jacobian matrix associated with linear velocities.

If the vector W represents the angular velocity of a coordinate frame located at the end effector within the simulator, then the representation:

$$W = J2 \ (d/dt) \ \Theta \tag{13}$$

is appropriate to describe the rotational velocities in Cartesian space. Here J2 is another 3x3 manipulator Jacobian matrix associated with the rotational velocities. Combining equations (12,13), it is seen that:

$$\begin{bmatrix} V \\ W \end{bmatrix} = \begin{bmatrix} J1 \\ J2 \end{bmatrix} (d/dt) \ \Theta = J \ (d/dt) \ \Theta \tag{14}$$

where J is defined as the overall 6x3 manipulator Jacobian for this system. J can be calculated in a variety of ways (Orin and Schrader, [7]).

This report addresses the application of the motion simulator to disorientation studies where the principal focus involves the orientation Jacobian J2. Figure 3 illustrates the body centered coordinate system located at the end effector in which all the final motion calculations, involving rotations and linear accelerations, are performed.

In the work considered herein, two minimum Coriolis inverse kinematics algorithms are considered to drive the motion simulator. The first algorithm contains zero Coriolis; the second algorithm minimizes the Coriolis. The purpose of the development of these algorithms is to modify the input kinematic commands of a motion simulator, similar to a centrifuge, to make the resulting motion fields more realistic to humans.

Calculation of Coriolis Induced on the DES

As mentioned previously, let W(t) represent the total angular velocity of the third, fixed body (the cab) desired at the end point of the motion simulator in Figure 1. This report addresses just the orientation problem to illustrate the procedure. For a three axes centrifuge motion simulator (modeled as a robot), one could express the 3x1 vector (d/dt) W(t) (the total vector of angular accelerations) measured in the same coordinate frame as W(t) in terms of the unit vectors of the inertial frame (i_0,j_0,k_0) in the following manner:

$$(d/dt)W(t) = [A3(t) \ i_0 \ , \ B3(t) \ j_0, \ C3(t) \ k_0]^T \tag{15}$$

where it can be shown that for the centrifuge simulator:

$$\begin{aligned} A3(t) = \ & (d^2/dt^2)\Theta_2 \ c1 - (d/dt)\Theta_2 \ [(d/dt)\Theta_1] \ s1 \\ & -(d^2/dt^2)\Theta_3 \ s1 \ c2 - (d/dt)\Theta_3 \ [(d/dt)\Theta_1] \ c1 \ c2 \\ & + (d/dt)\Theta_3 \ [(d/dt)\Theta_2] \ s1 \ s2 \end{aligned} \tag{16}$$

$$B3(t) = -(d^2/dt^2)\Theta_2\ s1 - (d/dt)\Theta_2\ [(d/dt)\Theta_1]\ c1 - (d^2/dt^2)\Theta_3\ c1\ c2 + (d/dt)\Theta_3\ [(d/dt)\Theta_1]\ s1\ c2 + (d/dt)\Theta_3\ [(d/dt)\Theta_2]\ c1\ s2 \quad (17)$$

$$C3(t) = -(d^2/dt^2)\Theta_1 - (d^2/dt^2)\Theta_3\ s2 - (d/dt)\Theta_3\ [(d/dt)\Theta_2]\ c2 \quad (18)$$

where $\Theta_{(i)}$, i=1,3 is a vector describing the joint angles of the centrifuge simulator and si and ci refer to sine and cosine, respectively. The orientation Jacobian matrix J2 was defined in equation (13) and the inverse kinematics relationship for orientation commands by which the joint angles can be integrated forward (since W(t) is specified a priori) is given by:

$$(d/dt)\ \Theta = [J2]^{-1}\ W \quad (19)$$

which is the inverse kinematics solution of interest in this study. The assumption in this report is that the orientation Jacobian J2 remains in a reasonable full rank configuration. In [1] this problem was addressed where this assumption was relaxed.

It is noted that (d/dt) W(t) can be broken up into two terms:

$$(d/dt)W(t) = (d/dt)W_{nc}(t) + (d/dt)W_c(t) \quad (20)$$

where the subscripts nc and c refer to noncoriolis and Coriolis terms, respectively. For the motion simulation problem this can be more explicitly written in the inertial coordinate frame:

$$(d/dt)W_c(t) = [AB3(t)i_0,\ BB3(t)j_0,\ CB3(t)k_0]^T \quad (21)$$

and the expressions for AB3, BB3, and CB3 can be easily obtained from equations (16-18):

$$AB3(t) = -(d\backslash dt)\Theta_2\ [(d\backslash dt)\Theta_1]\ s1 - (d\backslash dt)\Theta_3\ [(d\backslash dt)\Theta_1]\ c1c2 + (d\backslash dt)\Theta_3\ [(d\backslash dt)\Theta_2]\ s1\ s2 \quad (22)$$

$$BB3(t) = -(d\backslash dt)\Theta_2\ [(d\backslash dt)\Theta_1]\ c1 + (d\backslash dt)\Theta_3\ [(d\backslash dt)\Theta_1]\ s1c2 + (d\backslash dt)\Theta_3\ [(d\backslash dt)\Theta_2]\ c1\ s2 \quad (23)$$

$$CB3(t) = -(d\backslash dt)\Theta_3\ [(d\backslash dt)\Theta_2]\ c2 \quad (24)$$

The efforts in this report will focus on equation (20) dealing with orientation variables because Coriolis is so easily quantified. This term is what predominately affects pilots in a motion simulator. It is now possible (assuming a finite time t in $[t_0, t_f]$) to define two optimization problems related to minimizing Coriolis accelerations (and their resulting forces) appearing at the endpoint of the motion simulator. When viewed within the context of an optimization control problem (Lee and Markus, [8], and Bryson and Ho, [9]), these problems are linear-quadratic in nature. In the next section, $\Theta_{(k)}$ performs the role of state vector

which is the adapted joint commands and p(t) is the control variable which needs to be determined. First the problem will be formulated in attitude space with a hard constraint of zero Coriolis to appear at the end effector.

A Means to Reduce Coriolis on the DES

Method 1 - Zero Coriolis in an Attitude Space

The first attempt at this problem is to find a time history $\Theta_k(t)$ which, for a robotic manipulator system, becomes the modified joint kinematic commands that give rise to zero Coriolis. In this case it is desired to solve the following optimization problem by minimizing JB_1 with respect to a scaler control variable p(t) where:

$$JB_1 = (1/2)\int_{t_0}^{t_f} [\,|| \Theta(z) - \Theta_k(z) ||^2_{R1} + (1 - p(z))^2 r2]\, dz \qquad (25)$$

Here, again, the variable Θ_k becomes the state vector and the control variable (or variable to be determined) is p(t). The time interval t in $[t_0, t_f]$ describes the time duration in which the solution is desired. If the motion simulator is viewed as a robotic system, then $\Theta(.)$ is a vector of joint angles that are desired and specified via equation (19) since W is known a priori. Θ_k represents the actual joint angle time histories resulting from joint motions with reduced Coriolis. p(t) will be defined as a result of the linear quadratic optimization procedure. Note R1 is a positive definite symmetric matrix, $r2 > 0$, and the norm denotes Euclidian norm. Minimizing JB_1 is subject to the dynamic constraint (the state vector equation for Θ_k which is dependent on the control variable p(t)):

$$(d/dt)\,\Theta_k = p(t)\,[J2]^{-1}\,W \qquad (26)$$

where p(t) (not equal to 1) is to be selected. Equation (26) can be numerically integrated forward to determine the commanded or kinematic commands $\Theta_k(t)$. If $p(t)=1$, then the solution of (26) is given by equation (19) and contains Coriolis. Note that $\Theta_k(t)$ is described via equation (26) since W(t) is specified a priori. The optimization of (25) subject to (26) also has a state variable path constraint during t in $[t_0, t_f]$ of the form:

$$(d/dt)W_c(t) = (d/dt)W_c(t)[\Theta_k(t), (d/dt)\Theta_k(t)] = 0 \qquad (27)$$

It is noted that the hard constraint on the attitude variable in equation (27) is what gives method 1 the classification as zero Coriolis in attitude space.

A second solution to this problem is as follows:

Method 2 - Minimum Coriolis in an Attitude Space

A second method to approach this problem is to determine a modified time history $\Theta_k(t)$ to produce a command signal for the three actuators of the motion simulator which involves some nonzero Coriolis, but reduced from the expression specified in equation (19). This approach to the problem differs from Method 1 because the main concern is the reduction of Coriolis precisely at the body axis system as it affects the human subject with respect to the orientation variables. This solution also allows for the existence of some nonzero Coriolis, which is the case in both the simulator, as well as the actual aircraft. In this formulation, the objective is to minimize JB_3 with respect to a variable p(t) where:

$$JB_3 = (1/2)\int_{t_0}^{t_f} [\,|\,|(d/dt)W_c\,[\Theta_k(z),(d/dt)\Theta_k(z)]\,|\,|^2_{R1} + (1-p(z))^2 r2]\; dz \qquad (28)$$

subject to the dynamic relationship:

$$(d/dt)\Theta_k = p(t)\;[J2]^{-1}\;W(t) \qquad (29)$$

Again, as in Method 1, the state vector becomes $\Theta_k(t)$ and the control variable is p(t). Note that $(d/dt)W_c$ is defined in equation (21) and thus known explicitly. Hence, in Method 1 there exists a hard constraint on the Coriolis terms. In Method 2, however, the optimization procedure is used to minimize these terms,but some artifact is permitted (resulting in the existence of nonzero Coriolis) through the tradeoff between the attitude variables and the joint commands. The appendix describes in detail the actual optimization procedures for each of the two solutions to these problems. These results are summarized in the next section.

Results of the Optimization Procedure

With reference to the appendix, using the assumption that the orientation Jacobian $J2(\Theta)$ was nonsingular and could be used as a simplification for the determination of the p(t) equation (if not, $J2(\Theta_k)$ would be a more accurate approximation,or some damped least squares method could be employed), it was also noted that in both solutions, the expression for p(t) was found to be of the form:

$$p(t) = 1 + (\text{Coriolis reduction term}) \qquad (30)$$

because if p=1, then full Coriolis exists. The second term in equation (30) must reduce the Coriolis. This second term was found to be (in the solution of both optimization problems):

$$\text{Coriolis reduction term} = -(r2)^{-1}\ L^T\ (J2)^{-1}\ W \qquad (31)$$

where L is an adjoint variable which will be eliminated in the ensuing analysis.

Thus, by judiciously selecting r2, one can adjust the Coriolis effects to be made arbitrarily small. Of course, a tradeoff would then exist between minimization of the Coriolis terms compared to deviations of Θ_k from the desired Θ values.

To illustrate the applicability of this approach, the second method will be investigated via a computer study of the mathematical model describing the motion simulator (centrifuge).

Simulation Results

Applicability of The Approach to a Motion Simulator:

To apply this approach to a motion simulator, it is first required to have available the orientation Jacobian for the centrifuge simulator with respect to the body axis system in Figure 3. In (Repperger, [1,6]), The J2 (Orientation Jacobian) was determined:

$$J2 = \begin{matrix} s_{sy}c_{st}, & -s_{st}\ c1+c_{sy}c_{st}s1, & s1c2s_{st}+c1c2c_{sy}c_{st}+s2s_{sy}c_{st} \\ & -c_{sy}, & s1\ s_{sy}, \quad c1\ c2\ s_{sy} - c_{sy}\ s2 \\ -s_{sy}s_{st}, & -c1c_{st}- s1c_{sy}s_{st}, & s1c2\ c_{st}-c1c2c_{sy}s_{st} -s2\ s_{sy}\ s_{st} \end{matrix} \qquad (32)$$

where the subscripts sy and st again refer to the seat yaw rotation and seat back angle, respectively as depicted in Figures 1,3. For the example chosen in this report, the choice is made of Θ_{sy}= Pi/2, $\Theta_{st}=\Theta$. Geometrically this corresponds to the seat facing tangentially in the direction of rotation of the centrifuge.

For the seat configuration specified above, the Jacobian now becomes:

$$J2 = \begin{matrix} 1, & 0, & s2 \\ 0, & s1, & c1\ c2 \\ 0, & -c1, & s1\ c2 \end{matrix} \qquad (33)$$

To illustrate the applicability of this approach, it will be demonstrated on a special motion trajectory termed the "Cobra."

The Cobra is a "supermaneuver" (aircraft agility maneuver usually involving high angle of attack and post-stall motions) which has been demonstrated at airshows (Aviation Week, [10], and Cook, [11]) and has special significance in a combat scenario (cf. Figure 6).

When the lower aircraft performs this supermaneuver in Figure 6, it pitches up rapidly and slows down in the sky as a tactical ploy to confuse an opposing aircraft and to point first. As the lower aircraft translates along its velocity vector with its nose pitched up, it resembles a cobra snake ready to strike. It is simulated with the assumptions of 1000 feet altitude and a velocity change of from 300 Miles Per Hour to 150 Miles Per Hour. Most applications of this supermaneuver have been performed at low altitude and slow speed due to the potential structural damage to the aircraft during this flying procedure. The following commands on the joint motions of the centrifuge will emulate this motion:

$$\text{Roll Rotation} = \Theta_3(t) = (\text{Pi}/180)(30-2.5t) \text{ for } t \text{ in } [0,5]$$
$$= (\text{Pi}/180)*(5+2.5t) \text{ for } t \text{ in } [5,10] \quad (34)$$

$$\text{Yaw Rotation} = 0.0 \quad (35)$$

$$\text{Pitch Rotation} = -\Theta_2(t) = (\text{Pi}/3)*[1-\cos(\text{Pi}*t/5)] \quad (36)$$

$$\text{Arm Velocity} = (d/dt)\Theta_1(t) = 8.8-0.66t \text{ in RPM for } t \text{ in } [0,5] \quad (37a)$$

$$= 5.5 + 0.66(t-5) \text{ in RPM for } t \text{ in } [5,10] \quad (37b)$$

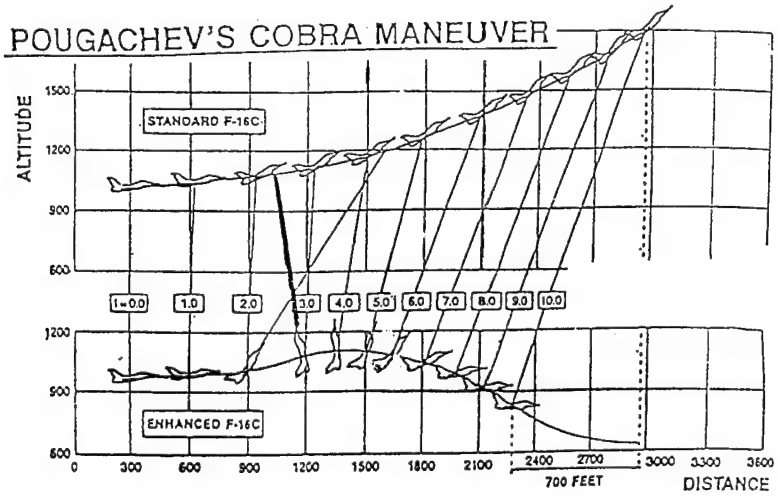

Figure 6. Pougochev's "Cobra" Supermaneuver

Note that the Θ_2 and Θ_3 variables have units of radians, but (d/dt) Θ_1 is in RPM. From equations (37a-b), it is obvious that (d/dt) Θ_1 being nonzero, is changing with time. Hence, this simulator has Coriolis because a frame (the fork = Θ_2, see Figure 1) rotates on another moving frame (the arm = Θ_1) and the cab = Θ_3 rotates on a moving frame (the fork = Θ_2). To calculate the magnitude of the Coriolis accelerations, it is necessary to mainly consider the inertial frame vector j_0 term. This term is the most disturbing to the pilot in this supermaneuver because it is in a direction (body axis Gy) to produce disorientation effects.

Table 3 lists the respective components of BB3 as specified in equation (23) for t in [0, 10]:

Table 3. Relative Components of BB3(t) for the Cobra Maneuver

	$(d/dt)\Theta_1 = W1$,	$(d/dt)\Theta_2$	$(d/dt)\Theta_3$
t in [0,5]	2.5-0.24t	$-(Pi^2/15)[\sin(Pi\ t/5)]$	-0.105
t in [5,10]	1.3+0.24t	$-(Pi^2/15)[\sin(Pi\ t/5)]$	0.105

Using equation (23) for BB3, Figure 7 illustrates the Coriolis acceleration for this supermaneuver versus time for t in [0,10]. The units for the dependent variable are Gy (1 Gy = 32.2 ft./s/s). From Figure 7 it is seen that the pilot experiences a Coriolis Gy of over $\pm$ 1.0 Gy during this supermaneuver. This is a sufficiently large value of motion artifact, as perceived by the pilot, as to make the centrifuge simulation unrealistic.

To correct this situation, the joint commands will be integrated forward using equation (29) and an optimization procedure is applied similar to Method 2 with the objective of minimizing Coriolis in attitude space. For the objective function JB_3 in equation (28), the choice is made of R1 = 2I, r2 = 8, 1, and 0.2. This results in the following two point boundary value problem:

$$L(t_f) = 0 \tag{38}$$

$$(d/dt)L^T = -(1/2) * (d/d\ \Theta_k)[(d/dt)W_c^T\ R1\ (d/dt)W_c] \tag{39}$$

$$p(t) = 1 - (r2)^{-1}\ L^T\ (J2)^{-1}\ W \tag{40}$$

$$(d/dt)\Theta_k = p\ (J2)^{-1}\ W(t) \tag{41}$$

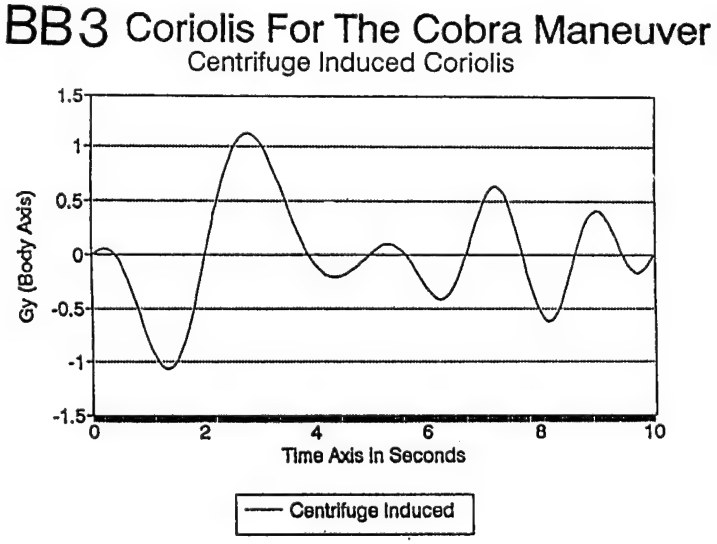

Figure 7. B Bar 3 Coriolis for the Cobra Supermaneuver

It is noted that the term $-(1/2)*(d/d\ \Theta_k)[(d/dt)W_c^T\ R1\ (d/dt)W_c]$ is obtained from equation (23) for BB3 = $(d/dt)\ W_c$. This assumption is made because the main concern is to minimize accelerations in the lateral Gy direction for each of the L(t) components. The Gy component is the most disturbing to humans and it is desired here to change the influencing functions L(t) as per this Gy component. If the interest was to reduce Coriolis effects in the other two axes, it would be a simple process to include the terms AB3 and CB3 in the ensuing analysis. The equations for the L(t) variables now become (with the assumption that R1 is diagonal with diagonal elements r1):

$$(d/dt)L_1 = -(1/2) * ((d/d\ \Theta_{1k})\ r1\ [BB3]^2) \tag{42}$$

$$(d/dt)L_2 = -(1/2) * (d/d\ \Theta_{2k})\ r1\ [BB3]^2 \tag{43}$$

$$(d/dt)\ L_3 = 0 \tag{44}$$

$$L(t_f) = 0 \tag{45}$$

The differential equation for L_3 has zero on the right hand side due to the independence of AB3, BB3, and CB3 on Θ_3. Since the vector $L(t_f) = 0$, this leaves L_1 and L_2 as the only nonzero variables. The relationship for BB3 is substituted from equation (23) and the partial differentiation is first taken and then the adjoint equations are then integrated backwards. Since:

$$(d/dt)\ \Theta_k = p(t)\ [J2]^{-1}\ W(t) \tag{46}$$

and:

$$p(t) = 1-\ (r2)^{-1}\ \ L^T\ \ \ (J2)^{-1}\ \ W \tag{47}$$

This corrects the Θ_i terms. The Θ_i are then integrated one step forward to obtain their respective corrections. The Coriolis can then be recalculated with these changes in the joint commands.

Figure 8 illustrates $L_2(t)$, the adjoint variable plotted for the case R1=2I. Figure 9 is a plot of the optimal control gain p(t) for the case r2=0.2. In Figure 10, plots of the term BB3 are illustrated for the choice of the original Coriolis and r2=1 which was the optimum weighting selected from this numerical study. From Figure 10 it is seen that a substantial reduction of Coriolis is possible. Comparing over time the sum of the squares of the BB3 terms, the minimum Coriolis is calculated for r2=1.0 and compared to the original Coriolis (resulting in a 65.4 percent reduction in Coriolis accelerations in the Gy direction produced by the motion simulator when it adapts these inverse kinematics algorithms).

If the Coriolis component is reduced, there exists a tradeoff in the adapted kinematic commands Θ_k from the desired commanded joint time history $\Theta(t)$. Examining equation (28) with the two weighting matrices R1 and r2 and utilizing the fact that the vector $\Theta(t)$ is 3x1, the cost (in a norm sense) of reducing this Coriolis component was determined to produce a compromise in the joint fidelity commands of only 5.1 percent. This amount of loss of motion fidelity may not be perceived by humans in this complex acceleration environment.

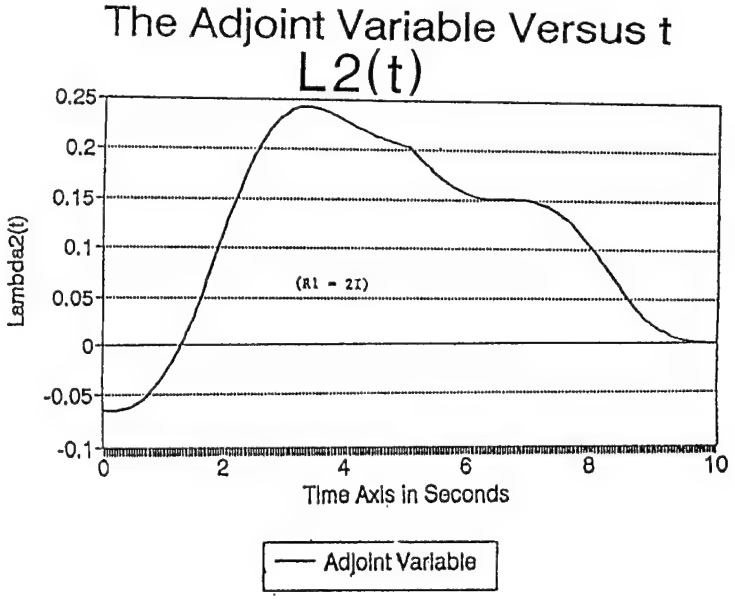

Figure 8. The Adjoint Variable Versus Time - Lambda 2 (t)

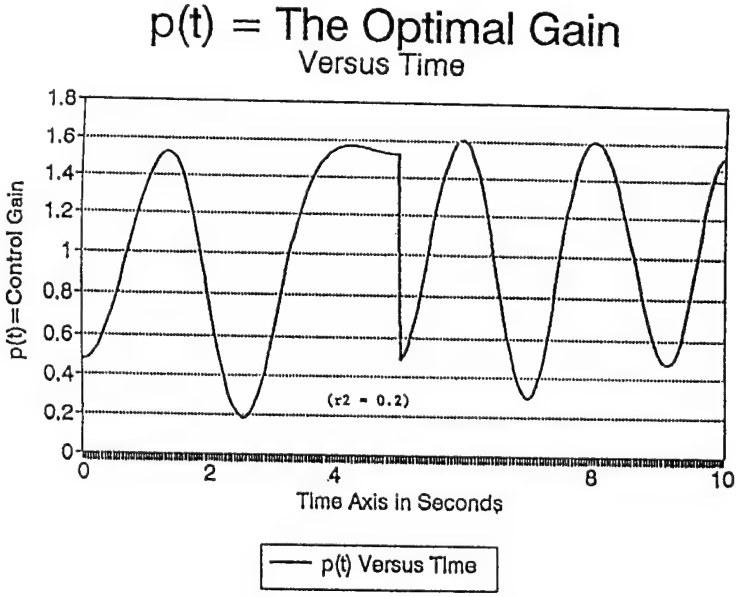

Figure 9. p(t) - The Optimal Gain Versus Time

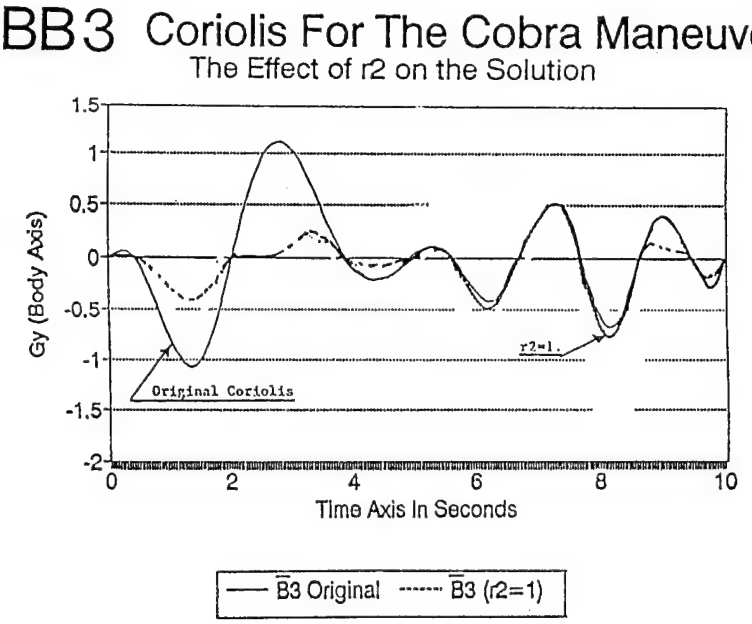

Figure 10. B Bar 3 Coriolis for the Cobra Supermaneuver - The Effects of r2 on the Solution

SUMMARY AND CONCLUSIONS

A three axis motion simulator is modeled as a robotic manipulator. The equations of motion are derived and the terms due to Coriolis are quantified. Two optimization algorithms are presented to minimize the Coriolis produced in the simulator at the end effector. It is shown with minimal reduction of motion fidelity, that over 65% of Coriolis can be reduced with proper input commands to modify the motion field produced. When this reduction of Coriolis is realized, the motion fidelity is only compromised about 5% which may not be perceivable by the human subjects that participate in the human runs in the mechanical system considered herein.

REFERENCES

[1] D. W. Repperger, "A Study of Supermaneuverability Flight Trajectories Through Motion Field Simulation of a Centrifuge Simulator," Transactions of the ASME Journal of Dynamic Systems, Measurement, and Control, Vol. 114, June 1992, pp. 270-277.

[2] D. W. Repperger, "Inverse Kinematic Control Algorithms With A Reduced Coriolis Component For Use In Motion Simulators," Transactions of the ASME Journal of Dynamic Systems, Measurement, and Control, to appear, 1995.

[3] D. W. Repperger and W. B. Albery, Patent # 5,353,226, "Coriolis Indicator for Situational Awareness," October 4, 1994.

[4] J. J. Craig, Introduction to Robotics, Addison-Wesley Publishing Company, Inc., 1986.

[5] D. W. Repperger, D. W., M. Z. Huang, and R. G. Roberts, "Dynamic Controller Design for a Fixed Base Motion Simulator," Proceedings of the 1994 American Control Conference, pp. 2298-2302, 1994.

[6] D. W. Repperger, "Determination of a Simulator's Capability Using Work Volume Techniques," 1990 American Control Conference, pp. 2063-2068, 1990.

[7] D. E. Orin, and W. W. Schrader, "Efficient Computation of The Jacobian For Robot Manipulators," The International Journal of Robotics Research, Vol 3, No. 4, Winter, pp. 66-75, 1984.

[8] E. B. Lee and L. Markus, "Foundations of Optimal Control Theory," Robert E. Krieger Publishing Company, Malabar, Florida, 1986.

[9] A. E. Bryson, and Y-C Ho, "Applied Optimal Control," Ginn and Company, 1969.

[10] Aviation Week and Space Technology, "British Pilot Lauds Performance of SU-27," 1990, pp. 35-40.

[11] W. J. Cook, "Turning on a Dime in Midair," US News and World Report, February 1989, pp. 56-58.

APPENDIX

Method 1 falls within the context of a linear quadratic optimization problem with path constraints along the optimal trajectory (Bryson and Ho, [9]). Method 2 is also a quadratic optimization problems, with the control entering in a linear manner. We now reformulate each optimization problem, defining the state variables, the control, and the procedure to solve each problem.

Method 1 - Minimize with respect to the control variable p(t):

$$JB_1 = (1/2)\int_{t_0}^{t_f} || \Theta(z) - \Theta_k(z) ||^2_{R1} + (1 - p(z))^2 \, r2 \, dz \tag{48}$$

where the state variable dynamic constraint is specified by:

$$(d/dt) \quad \Theta_k = p(t) \; [J2]^{-1} \; W \tag{49}$$

and state variable path constraint is given by:

$$C = (d/dt)W_c(t) = (d/dt)W_c(t)[\Theta_k(t),(d/dt)\Theta_k(t)] = 0 \tag{50}$$

The solution of this problem is specified once the Hamilitonian H(.) is chosen. For this case:

$$H = 1/2 * ((\Theta-\Theta_k)^T \, R1 \, (\Theta-\Theta_k)^T) + (1/2)* (1-p)^2 \, r2 + L^T [p \, (J2^{-1})] \, W + nu \, C \tag{51}$$

where the L(t) vector is the adjoint state variable and nu(t) is another influencing function chosen to deal with the equality constraint in equation (50). It is noted that in equation (49) the control p is linear in the state equation, and that W(t) and Θ(t) are known and specified a priori. The necessary conditions for optimality require:

$$(d/dt) \; L^T(t) = - H_{\Theta k} \tag{52}$$

with transversality condition:

$$L(t_f) = 0 \tag{53}$$

Thus:

$$(d/dt) \; L^T = - (\Theta-\Theta_k)^T \; R1 - nu \; (d/d \; \Theta_k) \; [C] \tag{54}$$

The second necessary condition is:

$$H_p = 0 \tag{55}$$

which yields:

$$(p\text{-}1) \quad r2 \; + \; L^T \; (J2)^{-1} \; W = 0 \tag{56}$$

which results in:

$$p(t) = 1 - \; (r2)^{-1} \; L^T \; (J2)^{-1} \; W \tag{57}$$

Thus, a two point boundary value problem is established in which the adjoint equations for L(t) are integrated backwards using equations (53) and (54) with p(t) is calculated forward from equation (57). Interestingly enough: p=1+ (a second term). If p=1, then Coriolis is present. The second term must be the Coriolis reduction term which adds linearly. The solution for problem 2 is now presented because it minimizes the Coriolis in the motion field directly experienced by the human subject. It also allows for some nonzero Coriolis artifact which is the case for the simulator, as well as in the actual aircraft.

Method 2 - Minimize with respect to the control variable p(t):

$$JB_3 = 1/2 \int_{t_0}^{t_f} \left| \left| d/dt(w_c)[\Theta_k(s),(d/ds)\ \Theta_k(s)] \right| \right|^2_{R1} + (1- p(s))^2\ r2\ ds \tag{58}$$

subject to a dynamic constraint on the state variables of the form:

$$(d/dt)\ \Theta_k = \; p(t)\ [J2]^{-1} \; W \tag{59}$$

For this case a Hamilitonian is defined as follows:

$$H = 1/2\ (d/dt)W_c^T\ R1\ (d/dt\ (W_c)) \; + \; 1/2\ (1\text{-}p)^2 r2 \; + \; L^T[p(J2)^{-1}W] \tag{60}$$

The necessary conditions for optimality require:

$$(d/dt)L^T(t) \; = \; - \; H_{(\Theta k)} \tag{61}$$

with transversality condition:

$$L(t_f) = 0 \tag{62}$$

Thus:

$$(d/dt)\, L^T = -1/2\, (d/d\Theta_k)[(d/dt)\, (W_c)^T\, R1\, (d/dt)\, W_c] \tag{63}$$

The second necessary condition ($H_p = 0$) yields:

$$(p\text{-}1)\ r2 + L^T\ (J2)^{-1}\, W = 0 \tag{64}$$

hence the familiar control law results (identical to equation (57)):

$$p(t) = 1 - (r2)^{-1}\, L^T\ (J2)^{-1}\, W \tag{65}$$

since $(d/dt)W_c(\Theta_k)$ is known (cf. equations (21-24)), this problem is easily solved.

Finally it is noted that it has been assumed that $(J2[\Theta])^{-1}$ is approximately $(J2[\Theta_k])^{-1}$ to eliminate the complexity of this factor into the analysis. If the $(d/d\ \Theta_k)\ (J2)^{-1}$ term were to appear in any of the L(t) equations, the problem becomes increasingly more difficult.

U. S. Government Printing Office 1995 650-075/00115